

## Supplementary information

### Synthesis, structure and properties of bimetallic sodium rare earth (RE)

#### borohydrides, $\text{NaRE}(\text{BH}_4)_4$ , RE = Ce, Pr, Er or Gd.

SeyedHosein Payandeh GharibDoust<sup>a</sup>, Dorthe B. Ravnsbæk<sup>b</sup>, Radovan Černý<sup>c</sup> and Torben R. Jensen<sup>a\*</sup>

<sup>a</sup>Department of Chemistry and Interdisciplinary Nanoscience Center (iNANO), Aarhus University, Langelandsgade 140, 8000 Aarhus C, Denmark.

<sup>b</sup>Department of Physics, Chemistry and Pharmacy, University of Southern Denmark (SDU), 5320 Odense M, Denmark

<sup>c</sup>Laboratory of Crystallography, Department of Quantum Matter Physics, University of Geneva, Quai Ernest-Ansermet 24, Geneva, Switzerland

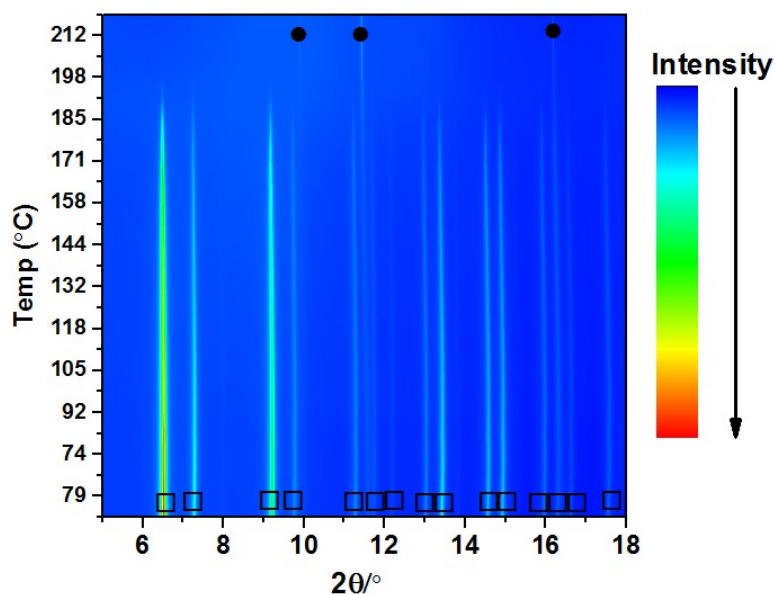


**Figure S1** *In-situ* SR-XRPD data for  $\text{Gd}(\text{BH}_4)_3\text{-NaBH}_4$  (1:1, s5).  $\Delta T/\Delta t = 5 \text{ }^\circ\text{C min}^{-1}$  (SLS,  $\lambda = 0.62177 \text{ \AA}$ )

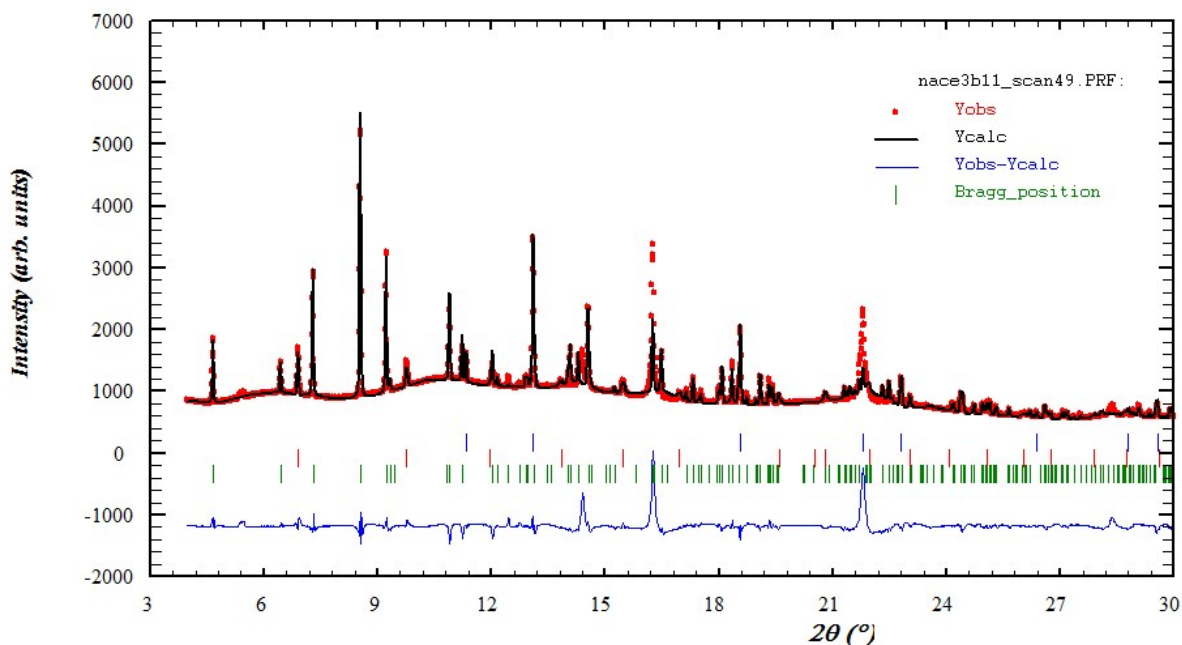


**Figure S2** XRPD pattern and refinement for  $\text{Ce}(\text{BH}_4)_3\text{-NaBH}_4$  (1:1, **s1**,  $\lambda = 0.7129$ ) recorded at 181 °C. Red line: experimental data; black line: calculated pattern, blue line: difference pattern. Sample composition: 1. Top, blue tick:  $\text{NaBH}_4$  (58.31 wt%). 2. Middle red ticks:  $\text{Ce}(\text{BH}_4)_3$  ( $Fm\bar{3}c$ , 3.08wt%) and 3. Bottom green ticks,  $\text{NaCe}(\text{BH}_4)_4$  (38.61 wt%).  $R_{\text{wp}} = 7.59\%$  (not corrected for background),  $\chi^2=359$ . The Bragg reflections that aren't refined are for the U2 phase.

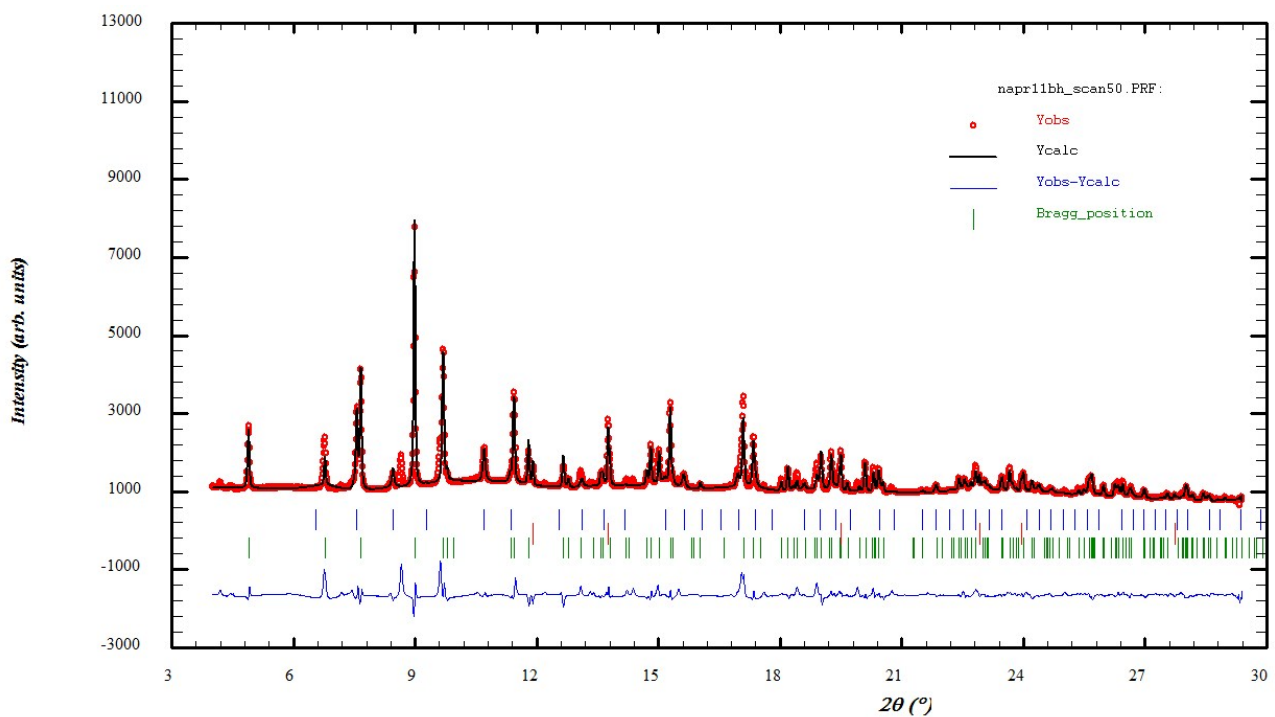


**Figure S3** XRPD pattern and refinement for  $\text{Pr}(\text{BH}_4)_3\text{-NaBH}_4$  (1:1, **s4**,  $\lambda = 0.7458$ ) recorded at 134 °C. Red line: experimental data; black line: calculated pattern, blue line: difference pattern. Sample composition: 1. Top, blue tick:  $\text{Pr}(\text{BH}_4)_3$  (16.48 wt%), 2. Middle red Ticks:  $\text{NaBH}_4$  (25.35 wt%), and 3. Bottom green ticks,  $\text{NaPr}(\text{BH}_4)_4$  (58.17 wt%).  $R_{\text{wp}} = 5.85\%$  (not corrected for background),  $\chi^2=319$ .

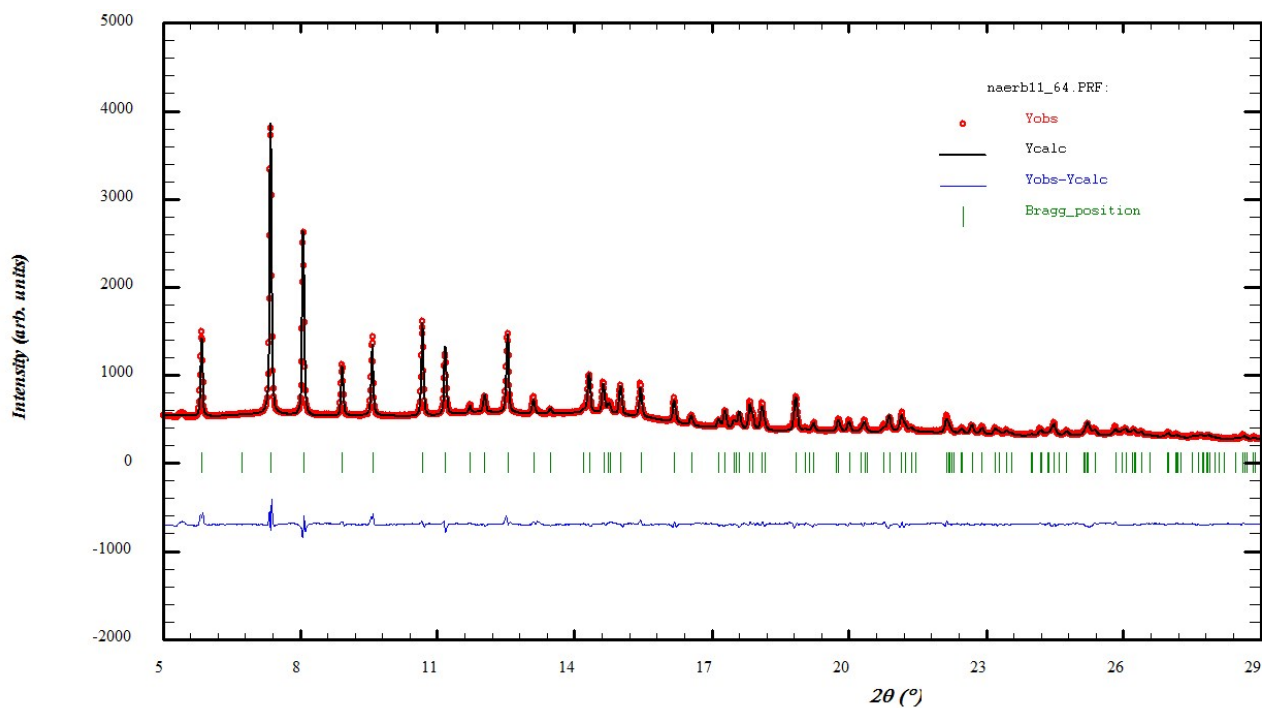


**Figure S4** XRPD pattern and refinement of  $\text{NaEr}(\text{BH}_4)_4$  (s7,  $\lambda = 0.7129$ ) recorded at  $122^\circ\text{C}$  (correct). Red line: experimental data; black line: calculated pattern, blue line: difference pattern.  $R_{\text{wp}} = 2.35\%$  (not corrected for background),  $\chi^2 = 190$ .

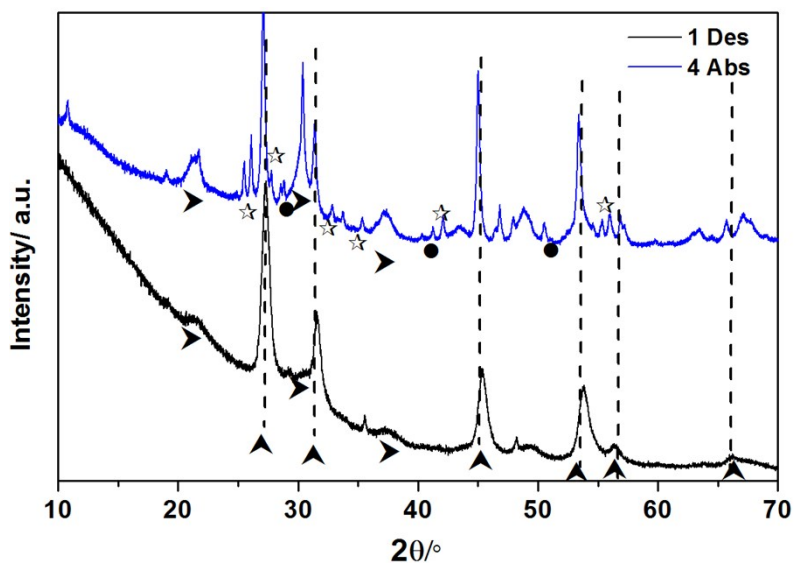


**Figure S5** XRPD patterns ( $\lambda = 1.54056 \text{ \AA}$ ) of  $\text{Ce}(\text{BH}_4)_3\text{-NaBH}_4$  (1 : 1, s1) after first decomposition (black curve) and fourth absorption (blue curve). Symbols:  $\text{⊙}$ ,  $\text{CeB}_6$ ;  $\text{⊗}$ ,  $\text{CeH}_{2+x}$ ;  $\bullet$ ;  $\text{NaBH}_4$  and  $\star$  for U5.

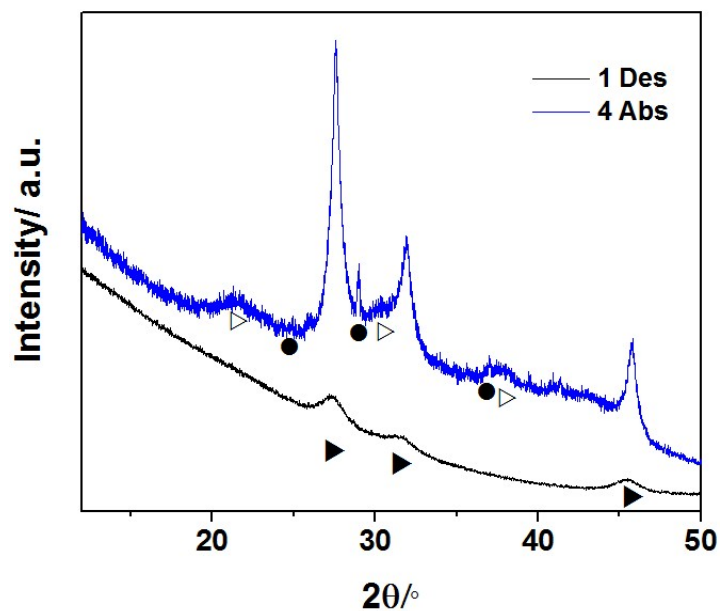


**Figure S6** XRPD patterns ( $\lambda = 1.54056 \text{ \AA}$ ) of Pr(BH<sub>4</sub>)<sub>3</sub>-NaBH<sub>4</sub> (1 : 1, s3) after first decomposition (black curve) and fourth absorption (blue curve). Symbols:  $\blacklozenge$ , PrB<sub>6</sub>;  $\blacklozenge$ , PrH<sub>2</sub> and  $\nabla$  for NaBH<sub>4</sub>.

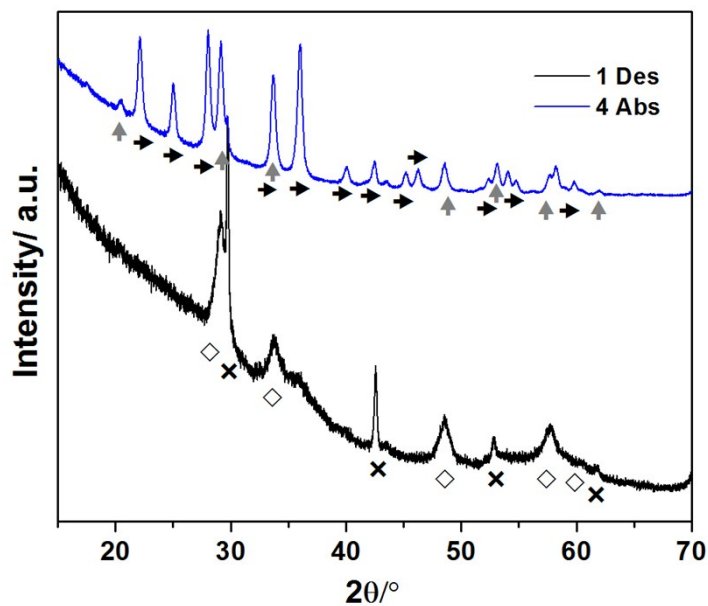


**Figure S7** XRPD patterns ( $\lambda = 1.54056 \text{ \AA}$ ) of Er(BH<sub>4</sub>)<sub>3</sub>-NaBH<sub>4</sub> (1 : 1, s7) after first decomposition (black curve) and fourth absorption (blue curve). Symbols:  $\ast$ , ErH<sub>2+x</sub>;  $\&$ , Na;  $\circ$ , ErB<sub>4</sub> and  $\bullet$  for Er<sub>2</sub>O<sub>3</sub>.

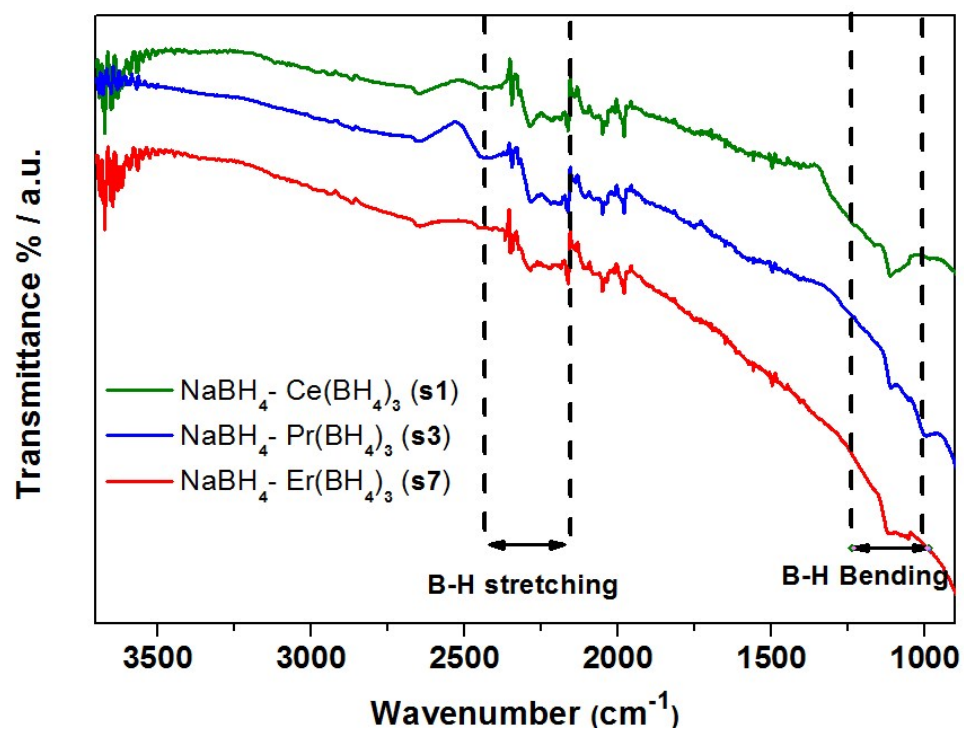


**Figure S8** FT-IR spectra of NaRE(BH<sub>4</sub>)<sub>4</sub>, RE = Ce, Pr, Er, after fifth absorption. The FT-IR spectra of NaBH<sub>4</sub> is also presented as a reference.

## Temperature programmed photographic analysis

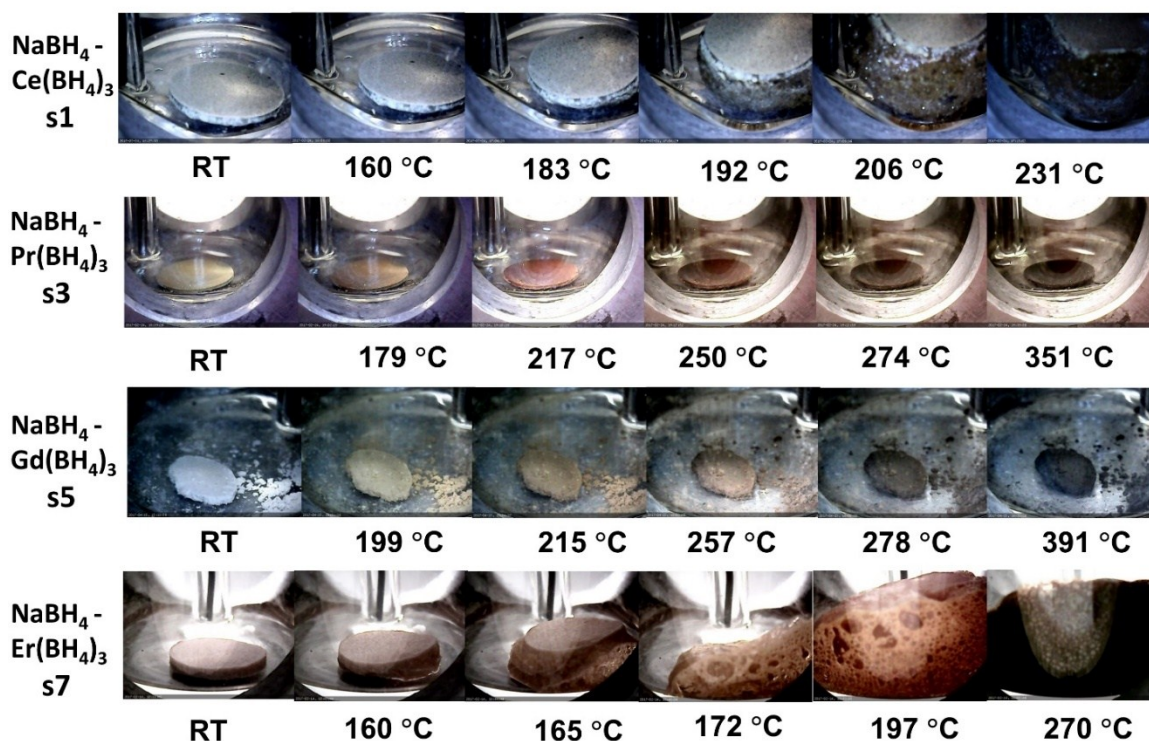


**Figure S9** Temperature programmed photographic analysis of samples **s1**, **s3**, **s5** and **s7** ( $\Delta T/\Delta t = 5$  °C/min, argon atmosphere).

The behaviors of the samples **s1**, **s3**, **s5**, and **s7** during heat treatment are investigated by temperature programmed photographic analysis (TPPA) and are displayed in Figure S10. NaBH<sub>4</sub> - Ce(BH<sub>4</sub>)<sub>3</sub> (1:1, **s1**) is a white powder at RT. At  $T \sim 170$  °C the sample starts to melt and foam, which corresponds to the maximum diffracted intensity of NaCe(BH<sub>4</sub>)<sub>4</sub> observed by *in-situ* XRPD. Foaming continues to  $T \sim 212$  °C and further heating of the sample leads to decomposition at  $\sim 230$  °C and the color change to black. The disappearance of the Bragg reflections at  $T = 187$  °C in the *in-situ* XRPD is associated with the melting/foaming of the sample.

$\text{NaBH}_4$  -  $\text{Pr}(\text{BH}_4)_3$  (1:1, **s3**) sample is light yellow at RT but changes to dark yellow at  $T \sim 170$  °C associated with the formation of  $\text{NaPr}(\text{BH}_4)_4$ . At  $T \sim 211$  °C, the pellet's color turns red, which corresponds to the formation of U4. At  $T > 250$  °C, the sample obtain a black color due to decomposition.  $\text{NaBH}_4$  -  $\text{Gd}(\text{BH}_4)_3$  (1:1, **s5**) sample is white at RT. The pellet shrinks and the sample's color changes to yellow at  $T \sim 199$  °C, which matches the formation of humps in the XRPD background data by quenching the sample at  $T \sim 205$  °C and suggests the formation of a new unstable compound, see Figure 1.b. At  $T > 270$  °C the sample turns black due to decomposition. TPPA shows that  $\text{NaBH}_4$  -  $\text{Er}(\text{BH}_4)_3$  (1:1, **s7**) is pink at RT and starts to melt/froth at  $T \sim 165$  °C and significant volume expansion occurs at  $\sim 190$  °C. At  $T > 216$  °C, the sample starts to decompose and obtain a black color.